Conformational Analysis of the α-L-Arabinofuranosides Present in Wheat Arabinoxylans from Proton-Proton Coupling Constants

R. A. Hoffmann,[†] J. van Wijk,[‡] B. R. Leeflang,[†] J. P. Kamerling,[†] C. Altona,[‡] and J. F. G. Vliegenthart*,[†]

Contribution from the Bijvoet Center, Department of Bio-Organic Chemistry, Utrecht University, P.O. Box 80.075, NL-3508 TB Utrecht, The Netherlands, and Gorlaeus Laboratories, University of Leiden, P.O. Box 9502, NL-2300 RA Leiden, The Netherlands. *Received September 6, 1991*

Abstract: The conformational behavior of α-L-arabinofuranosides present in wheat endosperm L-arabino-D-xylans has been investigated. To that purpose, oligosaccharides obtained by enzymatic digestion of a wheat endosperm L-arabino-D-xylan were submitted to *z*-filtered 1D homonuclear Hartmann-Hahn (HOHAHA) spectroscopy, and from the obtained vicinal proton-proton coupling constants, the ring conformation was deduced with the use of appropriate Karplus equations in conjunction with the concept of pseudorotation. The results revealed that α-L-arabinofuranosides linked to O3 of an internal *O*-3-mono- or *O*-2,3-disubstituted (1→4)-linked β-D-xylopyranose residue are present in a conformational equilibrium of equal amounts of ^4E-^4_0T (N-type) and ^1_2T-$_2E$ (S-type) conformers, whereas the α-L-arabinofuranoside linked to O2 of an internal *O*-2,3-disubstituted (1→4)-linked β-D-xylopyranose residue is present in a conformational equilibrium of equal amounts of ^4_3T-^4E (N-type) and ^1E-^1_2T (S-type) conformers. Both N- and S-type conformers of the investigated α-L-arabinofuranosides contain a rigid C4-O4-C1-O1 segment, assuming for O1 a pseudoaxial orientation and for the exocyclic CH_2OH group a pseudoequatorial orientation. From the proton-proton coupling constants the exocyclic rotamer populations could also be determined showing nearly equal preference for the g^- and *t* rotamers.

Introduction

Wheat arabinoxylans consist of a (1→4)-linked β-D-xylopyranose backbone with unsubstituted, *O*-3-monosubstituted, and *O*-2,3-disubstituted xylopyranose residues and single α-L-arabinofuranose groups.[1-3] They have a functional role in dough development and an influence on the baking performance of flour.[4,5] A prominent physical property of arabinoxylans is their high water-binding capacity,[6-8] which correlates with the molecular structure. For studies on the overall solution conformation of arabinoxylans, it is essential to have insight into the conformation of the constituent monosaccharides. So far, 3D information is only available with respect to the xylan backbone. ^1H NMR investigations of arabinoxylan oligosaccharides[9] showed that the β-D-xylopyranose residues present in the arabinoxylan backbone adopted the $^4C_1$ chair conformation. Here, the solution conformations of α-L-arabinofuranose residues (Figure 1) in two arabinoxylan oligosaccharides (**AX-31** and **AX-33**), obtained by *endo*-(1→4)-β-D-xylanase digestion of soluble wheat arabinoxylan,[9] are deduced from the vicinal ^1H-^1H coupling constants (^3J) with the use of appropriate Karplus equations in conjunction with the concept of pseudorotation.[10-12] This concept allows determination

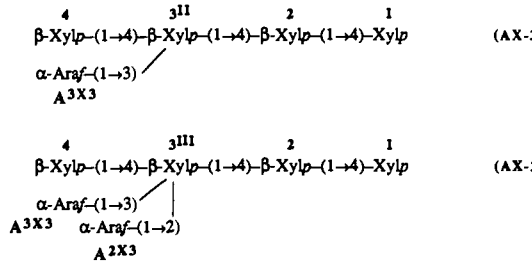

of the conformation of the furanose ring in terms of the phase angle of pseudorotation (*P*), the degree of pucker (Φ_m), and the conformational populations. To obtain pure absorption spectra containing only the arabinoxylan signals at high digital resolution, a 1D HOHAHA technique is applied which uses selective excitation and *z*-filtering.

Methods

Determination of Vicinal Coupling Constants from *z*-Filtered 1D HOHAHA Measurements. Prior to NMR spectroscopy, the arabinoxylan oligosaccharides **AX-31** and **AX-33** were repeatedly treated with ^2H_2O (99.9 atom % ^2H, MSD Isotopes) with intermediate lyophilization, finally using 99.96 atom % ^2H (MSD Isotopes) at $p^2H \geq 7$. Resolution-enhanced ^1H NMR spectra were recorded using a Bruker AM-500 spectrometer (Bijvoet Center, Department of NMR Spectroscopy, Utrecht University) at a probe temperature of 25 °C. Chemical shift values were measured by reference to internal acetone in ^2H_2O (δ 2.225).[13] The *z*-filtered 1D HOHAHA spin-lock experiments are carried out using the pulse sequence Sel_{270}-SL-90°$_\phi$-T_z-90°$_\phi$-acq, wherein SL stands for a multiple of the MLEV-17[14] sequence. For the selective excitation, a self-refocusing 270° gaussian pulse[15] of 144 ms was used. The spin-lock field strength corresponded to a 90° pulse width of 24 μs and a total spin-lock mixing time of 120 ms. To eliminate zero quantum coherence contributions, a *z*-filtering technique[16] was adopted consisting of two 90° pulses separated by "random" T_z values. The spectra were recorded with a spectral width of 2000 Hz and 8K data points, zero-filled to 32K. All ^1H NMR parameters for the α-L-Ara*f* residues were refined by spectral simulation at 500 MHz using an iterative spin simulation program, a minicomputer version of the Laocoon-type (5.0) programs, on a μ Vax II.[17]

Pseudorotation Analysis. The three degrees of conformational freedom available to furanosides that can be monitored by ^1H

[†] Utrecht University.
[‡] University of Leiden.

(1) Medcalf, D. G.; Gilles, K. A. *Cereal Chem.* **1968**, *45*, 550-556.
(2) Hoffmann, R. A.; Roza, M.; Maat, J.; Kamerling, J. P.; Vliegenthart, J. F. G. *Carbohydr. Polym.* **1991**, *15*, 415-430.
(3) Smith, M. M.; Hartley, R. D. *Carbohydr. Res.* **1983**, *118*, 65-80.
(4) Kühn, M. C.; Grosch, W. *Cereal Chem.* **1989**, *66*, 149-154.
(5) McCleary, B. V. *Int. J. Biol. Macromol.* **1986**, *8*, 349-354.
(6) Hanh, P. P.; Rasper, V. *Cereal Chem.* **1974**, *51*, 734-750.
(7) Kim, S. K.; D'Appolonia, B. L. *Cereal Chem.* **1977**, *54*, 225-229.
(8) Kühn, M. C.; Grosch, W. *J. Food Sci.* **1988**, *53*, 889-895.
(9) Hoffmann, R. A.; Leeflang, B. R.; De Barse, M. J.; Kamerling, J. P.; Vliegenthart, J. F. G. *Carbohydr. Res.* **1991**, *221*, 63-81.
(10) Altona, C.; Sundaralingam, M. *J. Am. Chem. Soc.* **1972**, *94*, 8205-8212.
(11) Altona, C.; Sundaralingam, M. *J. Am. Chem. Soc.* **1973**, *95*, 2333-2344.
(12) De Leeuw, F. A. A. M.; Altona, C. *J. Chem. Soc., Perkin Trans. 2* **1982**, 375-384.
(13) Vliegenthart, J. F. G.; Dorland, L.; Van Halbeek, H. *Adv. Carbohydr. Chem. Biochem.* **1983**, *41*, 209-374.
(14) Bax, A.; Davis, D. G. *J. Magn. Reson.* **1985**, *65*, 355-360.
(15) Emsley, L.; Bodenhausen, G. *J. Magn. Reson.* **1989**, *82*, 211-221.
(16) Subramanian, S.; Bax, A. *J. Magn. Reson.* **1987**, *71*, 325-330.
(17) Castellano, S.; Bothner-By, A. A. *J. Chem. Phys.* **1964**, *41*, 3863-3869.

0002-7863/92/1514-3710$03.00/0

Table I. ^{1}H NMR Chemical Shifts[a] and Vicinal ^{1}H–^{1}H Coupling Constants (in Parentheses)[b] of Protons of the α-L-Ara*f* Residues **A** (**AX-31**, A^{3X3}), **B** (**AX-33**, A^{3X3}), and **C** (**AX-33**, A^{2X3})

residue	H-1	H-2	H-3	H-4	H-5*R*	H-5*S*
A	5.397 (0.8)	4.160 (2.3)	3.907 (5.0)	4.272	3.798 (3.6)	3.717 (5.8, −12.2)
B	5.274 (1.0)	4.167 (2.5)	3.936 (5.4)	4.305	3.798 (3.5)	3.724 (5.6, −12.4)
C	5.224 (1.6)	4.150 (3.2)	3.959 (5.8)	4.130	3.818 (3.4)	3.722 (5.8, −12.3)

[a] In ppm relative to internal acetone at δ 2.225 in ^2H_2O at 25 °C, acquired at 500 MHz. [b] In hertz; estimated error <0.1 Hz. In the H-5*S* column, the geminal $^2J_{5S,5R}$ is also given.

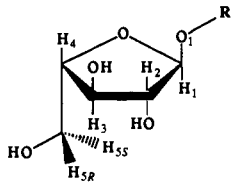

Figure 1. Structure of the α-L-arabinofuranose residues present in arabinoxylans. R stands for the (1→4)-linked β-D-xylopyranose backbone.

NMR spectroscopy comprise two related to the sugar ring (the pseudorotational phase angle *P* and the puckering amplitude Φ_m)[10] and one concerning the C4–C5 side chain (the exocyclic torsion angle ψ (O5–C5–C4–C3)[18,19]). The relation of the proton–proton torsion angles ($\Phi_{H,H}$) to the pseudorotational parameters in β-D-arabinofuranose rings[12] was used as starting point, taking into account the mirror-image pseudorotational itinerary of L-furanose rings with respect to that in the D series (Figure 2). For D-furanose rings, the standard N-type conformation ($P = 0°$) is defined as the conformation that has a maximal positive C1–C2–C3–C4 torsion angle, i.e., the $^2_3$T form. For L-furanose rings, the N-type is redefined as the form with the maximal negative value of the C1–C2–C3–C4 angle. This conformation will be denoted $^2_3$T to facilitate visualization, i.e., the present T, E notation refers to "up" and "down" in the same way as in the D series.

For the conversion of the β into the α configuration, it is assumed that the C1–H1 vector is phase-shifted by 120° with respect to C1–H1 in the β anomer. In this way, eq 4 in ref 12 is converted into eq 1 given here. Note that eq 1 yields the mirror image of an α-D configuration having the same values of Φ_m and *P*.

$\phi_{H,H}$ torsion angles in α-L-arabinofuranose:

$$\phi_{1,2} = 116.7° - 1.102\Phi_m \cos(P - 144°)$$

$$\phi_{2,3} = -120.2° - 1.090\Phi_m \cos P$$

$$\phi_{3,4} = 124.9° - 1.095\Phi_m \cos(P + 144°) \quad (1)$$

The torsion angles $\phi_{H,H}$ in eq 1 are linked to the corresponding proton–proton vicinal coupling constants by an extended Karplus equation[20] (an improved version of the one published by Haasnoot et al.[21]). The following relative electronegativities[20] are used for the substituents present on the C–C fragment along which the $^3J_{H,H}$ value is determined: H, 0; C, 0.62; O_H, 1.33; O_{ring}(O4), 1.40.

The experimental coupling constants $^3J_{exp}$ represent time average weighted values of *n* rapidly interconverting conformers that are linearly related to the coupling constants of the individual conformers ^3J_i and their populations X_i as expressed in eq 2.

$$^3J_{exp} = \sum_{i=1}^{n} X_i {}^3J_i \quad (2)$$

From ^{1}H NMR studies of nucleoside derivatives, it is well established[11,22] that the "flexible" D-furanose rings usually occur

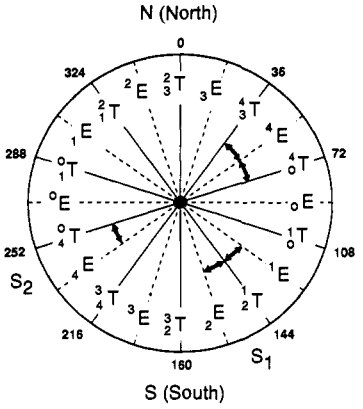

Figure 2. Pseudorotational pathway of the L-furanose ring. Each point on the circle represents a specific value of the phase angle of pseudorotation, *P*. Heavy radial lines represent twist (T) conformations; dotted radials represent envelop (E) forms. Heavy arrows indicate the preferred pseudorotational regions of the α-L-arabinofuranosides, whereby S_2 probably represents an artifact (see text).

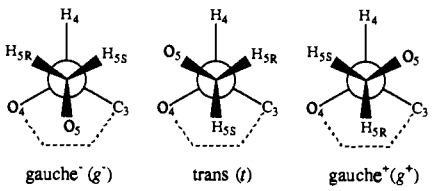

Figure 3. Three minimum energy (staggered) rotamers of the exocyclic CH_2OH fragment about the C4–C5 bond. Note that g^-, *t* and g^+ are defined with respect to the C4–C3 bond. The sign notation for the gauche rotamers is opposite to that used in the D series.

relative to the ^{1}H NMR time scale in a fast equilibrium between two conformations.[10,11,22] For L-furanose rings, two classes of conformers are distinguished: the N-type (phase angle of pseudorotation $-90° < P(N) < +90°$) and the S-type ($90° < P(S) < 270°$). With eqs 1 and 2 and the extended Karplus equation, the conformational parameters, *P*(N) and *P*(S), and the respective conformational population ratio X_N/X_S can be deduced from the three vicinal ring proton–proton couplings using the least-squares minimization program PSEUROT[22-24] (version 5.4). The puckering amplitudes $\Phi_m(N)$ and $\Phi_m(S)$ are kept fixed on values provided by X-ray structure analyses.

The conformation of the exocyclic CH_2OH fragment in terms of g^-, *t*, and g^+ rotamer populations (Figure 3) can be determined by analysis of the vicinal coupling constants $^3J_{4,5R}$ and $^3J_{4,5S}$. The rapid interconversion of the three rotamers in aqueous solution yields weighted time-averaged ^{1}H NMR coupling constants, which are related to the coupling constants $^3J^R$ and $^3J^S$ of the individual conformers and their corresponding populations by the following:

$$^3J_{4,5R} = X_{g^-}{}^3J^R_{g^-} + X_t{}^3J^R_t + X_{g^+}{}^3J^R_{g^+} \quad (3)$$

$$^3J_{4,5S} = X_{g^-}{}^3J^S_{g^-} + X_t{}^3J^S_t + X_{g^+}{}^3J^S_{g^+} \quad (4)$$

where X denotes the mole fractions of each of the conformers present ($\sum X_i = 1$). The coupling constants $^3J^R$ and $^3J^S$ for the

(18) Haasnoot, C. A. G.; De Leeuw, F. A. A. M.; De Leeuw, H. P. M.; Altona, C. *Recl. Trav. Chim. Pays-Bas* **1979**, *98*, 576–577.
(19) Wu, G. D.; Serianni, A. S.; Baker, R. *J. Org. Chem.* **1983**, *48*, 1750–1757.
(20) Donders, L. A. Ph.D. Thesis, University of Leiden, The Netherlands, 1989.
(21) Haasnoot, C. A. G.; De Leeuw, F. A. A. M.; Altona, C. *Tetrahedron* **1980**, *36*, 2783–2792.
(22) Haasnoot, C. A. G.; De Leeuw, F. A. A. M.; De Leeuw, H. P. M.; Altona, C. *Org. Magn. Reson.* **1981**, *15*, 43–52.
(23) De Leeuw, F. A. A. M.; Altona, C. *J. Comput. Chem.* **1983**, *4*, 428–437.
(24) De Leeuw, F. A. A. M.; Altona, C. *Quantum Chemistry Program Exchange*, 1983; No. 463.

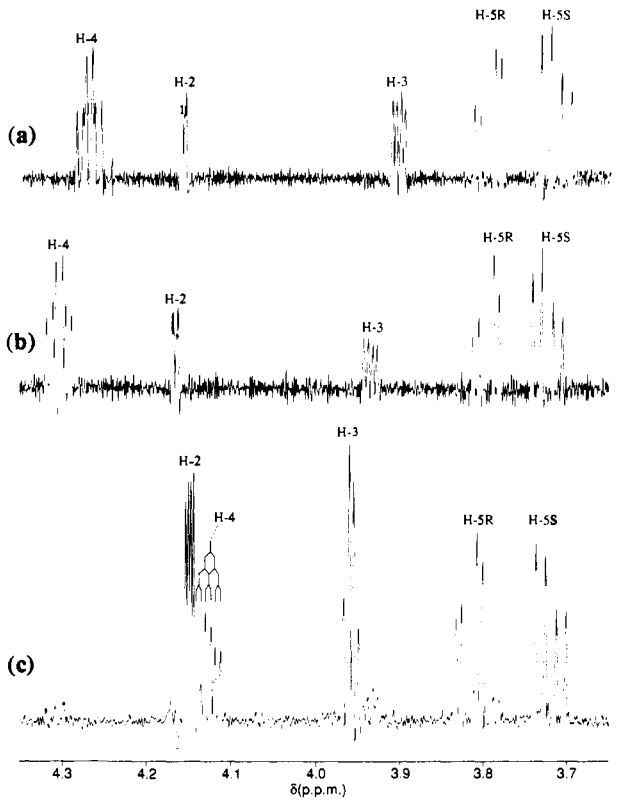

Figure 4. Resolution-enhanced 500-MHz 1D HOHAHA spectra of the three α-L-Ara*f* residues present in the two arabinoxylan oligosaccharides **AX-31** and **AX-33**. Only the relevant H-2–H-5 region is shown. The spectra were obtained by selective excitation of isolated arabinose signals, i.e., the H-4 signal of **A** (**AX-31**, A^{3X3}) at δ 4.272 (a) and of **B** (**AX-33**, A^{3X3}) at δ 4.305 (b) and the H-3 signal of **C** (**AX-33**, A^{2X3}) at δ 3.959 (c).

respective proton torsion angles $\phi_{4,5R}$ and $\phi_{4,5S}$ of the individual rotamers are calculated by means of an extended Karplus equation[20] using the appropriate $\phi_{H,H}$ torsion angles[18] (see Table III).

Results and Discussion

Determination of ^{1}H NMR Vicinal Coupling Constants. The ^{1}H NMR 1D HOHAHA spectra of the α-L-Ara*f* residues **A** (compound **AX-31**, A^{3X3}), **B** (compound **AX-33**, A^{3X3}), and **C** (compound **AX-33**, A^{2X3}) are given in Figure 4. The stereoselective assignment of H-5*S* and H-5*R* is done according to Wu et al.[19] on the basis of stereospecifically deuterated compounds. The resemblance of the spectra derived from the two (1→3)-linked α-L-Ara*f* residues is obvious. In the spectrum of the (1→2)-linked α-L-Ara*f* residue a large upfield shift of H-4 is seen (Table I).

To obtain pure vicinal ^{1}H–^{1}H coupling constants, stripped of any long-range couplings, the spectra are simulated, and the acquired values (J_{exp}) are compiled in Table I. The estimated error is less than 0.1 Hz.

Conformational Analysis of the Furanose Ring. Following well-established procedures, pseudorotational analyses are carried out for the three α-L-Ara*f* residues (^2H_2O, 25 °C) with the use of the experimentally determined coupling constant data. Since for each furanose ring five parameters influence three coupling constants, it is necessary to keep two parameters fixed during the least-squares iterative procedure. The problem now arises as to which of the five parameters are the two best candidates for constrainment to a fixed value, i.e., "best" in the sense that the most worthwhile information can be extracted from the data at hand. In the case of a strongly biased conformational equilibrium, the usual approach is to constrain the pseudorotation parameters of the minor component to previously determined standard values[25] in order to obtain the parameters of the more interesting major form. However, when both conformers are present in approximately equal amounts, another physically meaningful approach must be taken. Here, a statistical evaluation of knowledge gained from X-ray structure analysis can be called to our aid. From our previous experiences[25] in the field of β-D-ribonucleosides and -nucleotides, an excellent agreement exists between the ring puckering parameters Φ_m independently determined from X-ray analyses and those deduced from coupling constants by means of the PSEUROT program. Relevant to the present discussion is the finding that in all normal ribofuranosides encountered thus far (bicyclic structures excepted) Φ_m remains constant (mean value 39°) and appears from a statistical analysis to be independent of the nature of the nitrogen base substituent located at C1′.[12] A search in the Cambridge Structural Data Base System [copyright held by the Cambridge Crystallographic Data Centre, Cambridge, U.K.] for coordinates of arabinofuranosides published between 1972 and 1988 yields 27 independent X-ray determinations (bicyclic structures omitted), covering 25 different compounds. Four of these compounds carry a carbon substituted at C1, the remainder an aromatic nitrogen atom. The endocyclic torsion angles of the 27 arabinofuranose rings in our data set are calculated and subjected to a pseudorotation analysis.[10,25-27] It was found that in one instance[28] the published X-ray coordinates yielded the mirror-image geometry instead of the one investigated, and this error was corrected. Out of the 25 different arabinofuranoside rings, 14 forms crystallize in an N-type conformer ($-14° \le P(N) \le 52°$) and 11 in an S-type one ($105° \le P(S) \le 169°$).

Pertinent to the discussions presented below are the following observations: (a) the distribution of Φ_m values is remarkably narrow; (b) there exists no significant difference between the puckering amplitudes $\Phi_m(N)$ (38.2° ± 2.4°) and $\Phi_m(S)$ (39.0° ± 2.8°). Therefore, it appears appropriate to impose restrictions on the Φ_m parameters used in the PSEUROT analysis of the NMR couplings of the three α-arabinofuranoses:

$$\Phi_m(N) = \Phi_m(S) = \Phi_m$$

$$36° \le \Phi_m \le 40°$$

The PSEUROT program is first used in a series of pilot calculations designed to cover the complete conformational space of the pseudorotation pathway depicted in Figure 2. A two-state conformational model is assumed. The puckering amplitudes are kept fixed at the center of the known range: $\Phi_m(N) = \Phi_m(S) = 38°$.

The pseudorotational circle is divided into four quadrants: I ($0° \le P \le 90°$), II ($90° \le P \le 180°$), and so on. Four series of least-squares calculations are carried out for each of the three sets of available coupling constants of **A**, **B**, and **C**. In the first series of calculations for each set, a ring conformer is supposed to be present in quadrant I, $P(I)$ unknown, population unknown. $P(I)$ and the population ratio are treated as variables of the respective ranges, with starting values $P(I) \sim 45°$ and $X(I) \sim 50\%$. The remaining three quadrants are then systematically searched for acceptable solutions to the least-squares problem, i.e., minimizations are carried out for fixed values of $P(II)$ that are incremented from $P(II) = 90°$ to $P(II) = 360°$ in steps of 5°. In the second series, the conformer "to be refined" is placed in quadrant II, and $P(II)$ ranges over quadrants III, IV, and I. The third and fourth series cover possible solutions in quadrants III and IV. The resulting mass of solutions is analyzed in terms of the lowest root-mean-square (rms) deviations between observed and calculated coupling constants. In view of the estimated accuracy of the experimental couplings (<0.1 Hz), those regions in conformational space, where rms deviations of <0.3 Hz occurred, are selected for further study. The sets of coupling constants of the three α-L-Ara*f* residues give analogous, but not identical, results.

(25) Altona, C. *Recl. Trav. Chim. Pays-Bas* **1982**, *101*, 413–433.
(26) De Leeuw, H. P. M.; Haasnoot, C. A. G.; Altona, C. *Isr. J. Chem.* **1980**, *20*, 108–126.
(27) Huckriede, B. D.; Altona, C. Unpublished calculations.
(28) Hata, T.; Sato, S.; Kameko, M.; Shimizu, B.; Tamura, C. *Bull. Chem. Soc. Jpn.* **1974**, *47*, 2758–2763.

Table II. Calculated Pseudorotational Parameters and Molar Fractions X_N ($\Phi_m(N) = \Phi_m(S)$) of the α-L-Ara*f* Residues Present in the Arabinoxylan Oligosaccharides **AX-31** (**A**, A^{3X3}) and **AX-33** (**B**, A^{3X3}; **C**, A^{2X3}) at 25 °C

	A			B			C		
				S_1 Family					
$\Phi_m(N)$	36	38	40	36	38	40	36	38	40
$P(N)$	62.6	66.3	70.1	55.6	58.9	62.5	38.8	41.2	43.8
$P(S)$	153.7	155.4	158.6	143.3	143.7	144.9	134.2	133.3	132.7
X_N	0.53	0.53	0.54	0.52	0.52	0.52	0.53	0.51	0.50
rms[a] (Hz)	0.0	0.0	0.0	0.0	0.0	0.0	0.0	0.0	0.0
				S_2 Family					
$\Phi_m(N)$	36	38	40	36	38	40	36	38	40
$P(N)$	56.6	57.9	59.1	55.1	56.5	57.7	47.1	48.9	50.5
$P(S)$	234.3	235.6	236.5	240.1	241.0	241.6	250.6	251.3	251.8
X_N	0.55	0.54	0.52	0.59	0.58	0.56	0.64	0.62	0.61
rms[a] (Hz)	0.0	0.0	0.0	0.0	0.0	0.0	0.0	0.0	0.0
				S_1 Family					
$P(N)$		66 ± 4°, ^4E–$_0^4T$			59 ± 4°, ^4E–$_0^4T$			41 ± 3°, $_3^4T$–^4E	
$P(S)$		155 ± 4°, $_2^1T$–$_2E$			144 ± 2°, $_2^1T$			133 ± 1°, ^1E–$_2^1T$	
X_N		0.53 ± 0.01			0.52 ± 0.01			0.51 ± 0.02	
				S_2 Family					
$P(N)$		58 ± 2°, ^4E–$_0^4T$			57 ± 2°, ^4E–$_0^4T$			49 ± 2°, $_3^4T$–^4E	
$P(S)$		235 ± 2°, $_4E$			241 ± 1°, $_4E$–$_4^0T$			251 ± 1°, $_4^0T$	
X_N		0.54 ± 0.02			0.58 ± 0.02			0.62 ± 0.03	

[a] Root-mean-square deviation between observed and calculated coupling constants. The experimentally determined ^3J values and those obtained by PSEUROT were rounded off after completion of the PSEUROT calculations.

Surprisingly, two distinct families of—mathematically equivalent—solutions are obtained. The first family, denoted N/S_1, is characterized by an approximately 1:1 ratio of an N-type and an S_1-type conformer, wherein both conformers display phase angles *P*(N) and *P*(S) in the "classical ranges" $_3^4T$–$_0^4T$ and $_2^1T$–$_2E$ (Figure 2). The second family, denoted N/S_2, displays a classical N-type form in equilibrium with a nonclassical high S_2 conformer in the range $_4E$–$_4^0T$. No other solutions to the least-squares optimization problem are found.

In the next step, the two families of possible solutions are investigated more closely with the aid of PSEUROT. Three independent series of three calculations are carried out for each α-L-Ara*f* and for both families. The puckering amplitudes Φ_m are fixed in turn at 36°, 38°, and 40°, respectively, to estimate the correlation between Φ_m and the parameters "to be refined": *P*(N), *P*(S), and the conformational population ratio. In all cases a perfect rms match is obtained (Table II).

At this point, we stress the fact that the existence of two discrete mathematical solutions to a least-squares minimization does not necessarily imply that both solutions have equal probability. On the contrary, for reasons outlined below it appears likely that conformers belonging to the N/S_2 family represent artifacts.

The double-solution problem arises from the fact that for the α-L-arabinofuranose ring in the S_1- and S_2-type conformers (Table I) all three (trans) proton–proton torsion angles $\phi_{H,H}$ are close to 90°. For each of the three torsion angles this gives a minimum in the Karplus curve in plots of $^3J_{HH}$ versus $\phi_{H,H}$. For example, the PSEUROT calculation yields for **A** in the S_1 form, with *P*(S) 155.4° and Φ_m(S) 38° (fixed), the following $\phi_{H,H}$ values: $\phi_{1,2}$ = 75.6°, $\phi_{2,3}$ = −82.6°, $\phi_{3,4}$ = 104.5°. Thus, all three corresponding couplings are small (≤1.3 Hz). Pseudorotation to the S_2 form with *P*(S) 235.6° and Φ_m(S) 38° (fixed) yields $\phi_{1,2}$ = 117.8°, $\phi_{2,3}$ = −96.8°, and $\phi_{3,4}$ = 85.7°; again, the corresponding couplings are small (≤1.0 Hz). This explains why two different S-type conformers are obtained in conformational space. This situation appears to be connected to the all-trans position along each successive bond of α-L-arabinofuranoses. Small differences exist between S_1 and S_2 coupling constants, but these differences are easily compensated for by the small changes in the two remaining adjustable parameters, i.e., *P*(N) and the molar population ratio.

Although S_1 and S_2 are mathematically equivalent as far as the interpretation of the coupling constants is concerned, the two resulting conformers differ profoundly in their respective structural properties. Conformer S_1 has a priori favorable features, viz., a pseudoaxial OR substituent at C1, in agreement with considerations based on the anomeric effect,[29] and a stereochemically acceptable pseudoequatorial C5 side chain at C4. In contrast, form S_2 shows exactly opposite features (Figure 2), in addition to an apparently unfavorable 1,3-diaxial interaction between the C5 side chain and the axial OH group at C2.

These qualitative arguments are amplified with the aid of molecular mechanics and semiempirical calculations. The methyl α-L-arabinofuranoside (Figure 1, R = CH_3) is chosen as a model compound. The pseudorotational itinerary is explored with the aid of three different approaches: (1) AM1,[30] (2) a modified version of QUANTA/CHARMm 3.0,[31] and (3) MM2(85).[32] In all three series selected torsion angles are driven in a manner similar to that reported[33] for ribofuranoses. The AM1 approach is the least satisfactory in our case, since the furanose ring tends to flatten to unrealistically low puckering amplitudes (ca. 12°). This behavior appears to be related to the low torsion barriers calculated by Gundertofte et al.[34] The modification introduced in the CHARMm 3.0 force field concerns the addition of V_2 and V_3 torsion potential functions that properly account for the anomeric effect along C–O–C–O fragments; this modified torsion potential is based on ab initio calculations with the aid of a 6-31G* basis set.[35] Pilot calculations of the pseudorotational pathway, carried out for several preset values of the puckering amplitude ranging from 30° to 48°, clearly show that the conformational energy in the S_2 region (*P* 210°–270°) remains at least 1 kcal/mol higher than that calculated for the S_1 region (*P* 130°–160°). The MM2 calculations yield essentially the same picture as QUANTA/CHARMm. It is predicted that the S_2 region is destabilized by 1.0 kcal/mol relative to the S_1 domain. From the considerations it can be concluded that the S_2 forms probably can be dismissed as artifacts due to the α-L-arabinofuranoside stereochemistry.

(29) Kirby, A. J. *The Anomeric Effect and Related Stereoelectronic Effects at Oxygen*; Springer: Berlin, 1983.
(30) Dewar, M. J. S.; Zoebisch, E. G.; Healy, E. F.; Stewart, J. J. P. *J. Am. Chem. Soc.* **1985**, *107*, 3902–3909. The program is available from the Quantum Chemistry Program Exchange, University of Indiana, Bloomington, IN. QCPE Program No. 527 was used.
(31) Copyright Polygen Corp., Waltham, MA.
(32) Allinger, N. L. *J. Am. Chem. Soc.* **1977**, *99*, 8127. The program is available from the Quantum Chemistry Program Exchange, University of Indiana, Bloomington, IN. QCPE Program No. 395 was used in combination with the 1985 parameter set.
(33) Raap, J.; Van Boom, J. H.; Van Lieshout, H. C.; Haasnoot, C. A. G. *J. Am. Chem. Soc.* **1988**, *110*, 2736–2743.
(34) Gundertofte, K.; Palm, J.; Pettersson, I.; Stamvik, A. *J. Comput. Chem.* **1991**, *12*, 200–208.
(35) Huige, C. J. M.; Altona, C. Unpublished calculations.

Table III. Proton–Proton Torsion Angles (ϕ) of the Three Rotamers (g^-, t, and g^+) and the Corresponding Calculated Vicinal Coupling Constants in L-Arabinofuranose Residues. Also Given are the Calculated Relative Rotamer Populations in the Three α-L-Ara$f$ Residues **A** (**AX-31**, A^{3X3}), **B** (**AX-33**, A^{3X3}), and **C** (**AX-33**, A^{2X3})

rotamer	ϕ(H4,H5R)	J^R (Hz)	ϕ(H4,H5S)	J^S (Hz)	**A** (%)	**B** (%)	**C** (%)
g^-	64°	2.2	−55°	1.2	37	42	39
t	−64°	2.4	−178°	10.5	46	43	46
g^+	−174°	10.4	68°	3.6	17	14	15

Therefore, the discussion can be limited to the properties of the N/S_1 families.

From Table II it is seen that **A** and **B** display remarkably similar conformational behavior. Both furanose rings occupy the ^4E–^4_0T range (N-type) and the ^1_2T–$_2E$ range (S-type) in approximately equal amounts. Residue **C** displays a gradual difference in pseudorotational parameters: ^4_3T–^4E (N-type) and ^1E–^1_2T (S-type). The conformational equilibrium (~50/50) is thereby not affected. The actual choice of fixed ring puckering parameter Φ_m hardly influences the outcome of the PSEUROT calculation (Table II).

Manipulation of mechanical models reveals that the C5–C4–O4–C1–O1 part of the α-L-arabinofuranose skeleton tends to remain relatively unchanged in going from the N range to the S_1 range of conformations. This impression is corroborated by CHARMm force field calculations in which the five-membered ring is constrained to adopt the experimentally determined values, Φ_m = 38°, P(N) = 60°, P(S) = 150°; i.e., only the side chain atoms are allowed to vary. Inspection of the two resulting structures shows that the anomeric C4–O4–C1–O1 fragment of the α-L-arabinofuranoside remains fairly rigid: in going from N to S_1, torsion angle Φ(C5–C4–O4–C1) varies from −160° to −130°, whereas Φ(C4–O4–C1–O1) changes only from −95° to −89°.

Conformation of the Exocyclic, Primary CH_2OH Group. The proton–proton torsion angles for the three minimal energy (staggered) rotamers (g^-, t, and g^+) about the exocyclic C4–C5 bond of D-furanose systems have been taken from Haasnoot et al.[18] and adapted for the L isomers. These torsion angles, in combination with an extended Karplus equation,[20,21] yield the predicted limiting coupling constants compiled in Table III.

In aqueous solutions the rapid interconversion of the three rotamers yields weighted time-averaged ^1H NMR couplings of the individual rotamers and their relative populations. Using the measured time-averaged ^1H NMR coupling constants of the three α-L-Ara$f$ residues given in Table III in conjunction with eqs 3 and 4, the relative populations of the three rotamers could be determined and are collected in Table III. These data predict a nearly equal preference for the g^- and t rotamers. The dominance of the g^- and t rotamers, in which O5 is gauche to the ring oxygen (O4), can be rationalized by assuming a predominant gauche effect which, as defined by Wolfe,[36] means a strong preference for a gauche O–C–C–O orientation relative to a trans conformation of the corresponding fragment. Alternatively, it has been proposed that the gauche effect arises from a stereoelectronic preference of the most electronegative ligands on a C–C fragment to adopt a trans position with respect to the least electronegative ligands.[37] Moreover, in the g^- and t rotamers, an intramolecular hydrogen bond can occur between the C5 hydroxyl group and the endocyclic ring oxygen, but not in the g^+ rotamer. These results are consistent with the solution rotamer distribution found for methyl α-D-arabinofuranose,[19] indicating that the exocyclic CH_2OH part of the α-L-Ara$f$ residues present in the arabinoxylans does not interact specifically with the (1→4)-β-D-xylopyranose backbone.

From the data obtained it may be concluded that the α-L-Ara$f$ residues have a large amount of conformational freedom. This means a rapid equilibrium between almost equally populated conformational species. Both the N- and S-type conformers of the α-L-Ara$f$ residues contain a rigid C4–O4–C1–O1 segment with O1 in a pseudoaxial orientation and the primary exocylic CH_2OH group adopting a pseudoequatorial orientation. These results, together with knowledge of the xylan backbone conformation,[9,38] should make it possible, by the application of molecular mechanics and molecular dynamics programs, to generate more accurate models for further studies on the structure–function relation of plant cell wall arabinoxylans. Our conclusions extend and reinforce those reached by Serianni and Barker[39] on tetrofuranosyl ring conformations.

Acknowledgment. This work was supported by Unilever Research Vlaardingen with financial aid from the Dutch Ministry of Economic Affairs (ITP-program) and the Netherlands Foundation of Chemical Research (NWO/SON).

Registry No. AX-31, 84666-93-3; AX-33, 134507-64-5; arabinoxylan, 9040-27-1.

(36) Wolfe, S. *Acc. Chem. Res.* **1972**, *5*, 102–111.
(37) Baddeley, G. *Tetrahedron Lett.* **1973**, 1645–1648.
(38) Nieduszynski, I. A.; Marchessault, R. H. *Biopolymers* **1972**, *11*, 1335–1344.
(39) Serianni, A.; Barker, R. *J. Org. Chem.* **1984**, *49*, 3292–3300.